Asian Journal of Information Technology 17 (7-12): 321-327, 2018
ISSN: 1682-3915

A Simple Tool for Identifying the Severity of Alzheimer's Based on Hippocampal and Ventricular Size Using a Roc Curve on a Coronal Slice Image

[1]Retno Supriyanti, [1]Ays Rahmadian Subhi, [1]Yogi Ramadhani and [2]Haris B. Widodo
[1]Department of Electrical Engineering,
[2]Medical Faculty, Jenderal Soedirman University, Purwokerto, Indonesia

Abstract: Alzheimer's diagnosed early can make the patient have more time to prepare and plan for the future. One more important thing is getting faster handling. The doctor will suspect a patient suffering from Alzheimer's disease if questions answered by the patient around the symptoms his or her family's health history and life style leads to a disease other than Alzheimer's. But actually the most accurate way of diagnosing Alzheimer's disease is through an autopsy that allows the examiner to see the patient's brain tissue. At this time to perform an autopsy does not have to do with the patient's head surgery. One device that can be used to explore the head tissue is MRI. This study will discuss the development of computer aided diagnosis tool in identifying the severity of Alzheimer's using ROC curve, especially, for coronal slice image from MRI. In this experiment, we used the hippocampal and ventricle size parameters as the determinant variable of Alzheimer's severity with reference to the value of Clinical Dementia Rating (CDR). Pre-processing to get the value of variable size by using active contour method. The results show the accuracy level of hippocampal object identification of 98.4 and 86.3% ventricular object.

Key words: Alzheimer, coronal slice, ROC curve, severity, clinical dementia rating, identification

INTRODUCTION

Dementia is a general term, describing the symptoms that occur when the brain is affected by a disease or condition. There are different types of dementia, although, some are more common than others because they are often named according to the conditions that have caused the dementia. Alzheimer's disease is the most common cause of dementia. During the illness, chemicals and brain structures are altered to cause death of brain cells. The term dementia describes a series of symptoms that include memory loss, mood swings, problems with communication and reasoning. These symptoms occur when the brain is damaged by a disease or certain conditions including Alzheimer's disease. All types of dementia move progressively. This means that the brain's chemical structure becomes increasingly damaged over time. A person's ability to remember, understand, communicate and think gradually decreases. The stage of severity in the dementia disease in medicine can be translated on a scale called the Clinical Dementia Rating (CDR) (Morris, 1993). As already mentioned that Alzheimer's is the most cause of dementia then in this study we will use the term Alzheimer's disease. The CDR scale scores provide a guide for physicians to diagnose the severity of Alzheimer's disease based on interview data and clinical diagnoses. In principle the CDR scale can be summarized into the following five states: 0 = Normal; 0.5 = Very mild dementia; 1 = Mild dementia; 2 = Moderate dementia; 3 = Severe dementia. But actually, the diagnosis of Alzheimer's can be done quickly by analyzing the human brain tissue, especially for the hippocampal and ventricle contained in the human brain. However, in analyzing the brain tissue is required very high precision from the physician. Whereas in reality not all physicians can always have a high accuracy, therefore, the error diagnosis because of human error can occur. One of devices that can be used to get a clear description of the tissues and organs in the human brain is using Magnetic Resonance Imaging (MRI) machine. In the image taking using MRI machine will be produced 3 types of slices namely coronal, axial and sagittal as shown in Fig. 1.

Referring to Fig. 1, the types of slices support each other in the determination of the diagnosis. According to this case, detailed analysis of each type of slice is required. The main purpose of our research is to develop computer aided diagnosis to perform automatic classification in determining the severity of Alzheimer's. This was carried out to handle the problem of the increasing number of Alzheimer's patients in Indonesia

Corresponding Author: Retno Supriyanti, Department of Electrical Engineering, Jenderal Soedirman University, Purwokerto, Indonesia

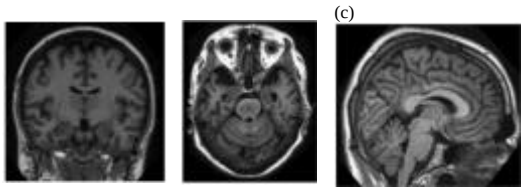

Fig. 1: Slice types in MRI image (OASIS database sets): a) Coronal; b) Axial and c) Sagittal

and other developing countries, especially in providing treatment for Alzheimer's sufferers. By knowing the level of Alzheimer's severity accurately and quickly, the patient can get maximum care. In developed countries with many doctors having high competence and supported by the availability of good quality MRI machines, the diagnosis of Alzheimer's severity is not a problem. But for developing countries like Indonesia, the existence of a simple and inexpensive yet accurate technological device that can support the diagnosis of severity becomes an important issue. While for research that has been done before about the classification of the severity of Alzheimer's there are some of them are as follows. Gray *et al.* (2012) conducted a research by combining cross-sectional and longitudinal FDG_PET multi-region information as a basis for classification. He used clinical data on images from the Alzheimer's disease neuroimaging initiative. Segmentation is carried out in 83 areas automatically and followed by monitoring changes in signal intensity in a certain period of time. Fu *et al.* (2014) conducted a research to identify the optimal time required to obtain preliminary information from some biomarkers that can be used in the image and serve as a basis for the classification of Alzheimer's. Tohka *et al.* (2016) conducted comparative split-half resampling analysis of various data feature options and classification methods for all analyzes on brain voxels based on anatomic magnetic resonance images. In comparing classification, he used the Support Vector Machine (SVM) method. Wee *et al.* (2012) in his study proposed a framework of pattern classification a high dimension based on a functional combination between brain regions at rest. This is done to identify the brain's abnormalities leading to Alzheimer's. The proposed technique used a multi-spectrum network to characterize the existing phase changes. Fiscon *et al.* (2018) in his research, he implements procedures for the exploration of feature and classification techniques on EEG signals. The primary goal is to distinguish patients affected by Alzheimer's Disease (AD) as influenced by Mild Cognitive Impairment (MCI) and Healthy Control (HC) samples. He performs a time frequency analysis by applying Fourier and Wavelet transforms to 3 types of AD, MCI and HC samples. Gerardin *et al.* (2009) in his research, he used the Spherical Harmonics coefficient (SPHARM) to model the segmented hippocampal shape using the previously developed automatic segmentation method. The primary goal of his research was to classify between patients with Alzheimer's Disease (AD) or Mild Cognitive Impairment (MCI) and elderly controls based on the hippocampal shape. Yun *et al.* (2015) proposed a new method to distinguish patients with Alzheimer's Disease (AD) and normal patients based on information that can be explored from MRI. In his new method, he used 12 predetermined areas in his previous research. In this case he used partial linear discriminant analysis to make the diagnosis. Wolz *et al.* (2011) he proposed methods for assessing the increase in classification accuracy that can be achieved by integrating features from different MRI structural analyzes. MRI features used are hippocampal volume, tensor morphology and cortical density. Dyrba *et al.* (2013) he applied multivariate Machine Learning (ML) to the data center of the framework he created himseif on the study of dementia. He estimates that the use of ML can change the effect of data center acquisition. He used 137 AD patients with 143 healthy elderly controls. For diagnostic classifications he used Fractional Anisotropy (FA) and average diffusivity (MD). Cho *et al.* (2012) he proposed a method of classifying Alzheimer's by using cortical thickness based on the manifold transformation of harmonics. Ye *et al.* (2016) he proposed a feature selection method to determine the most different features in the framework of AD/MCI multi-modal classification. For each modality, he trained the linear regression model using the appropriate modalities then proceeded to use group-sparsity algorithms for general feature selection on various modalities. Singanamalli *et al.* (2017) he presented a combined framework between the correlation of a canonical correlation multiview cascade as a classification of fusion and cascade that integrates all diagnostic categories and optimizes the classification by combining subsets of modalities at each level of cascade selectively. Huang *et al.* (2017) he presented a longitudinal measurement of the MCI brain image and hierarchically made a classification method for predictions of Alzheimer's. Longitudinal images were obtained individually in MCI patients and further investigated to obtain information on longitudinal phase changes. Belloy *et al.* (2018) in his study, he stated that QPP will provide information about DMN and TPN FC that deviates in people with Alzheimer's. According with this then the feature can be used as a biomarker that is more sensitive in the classification of Alzheimer's. As we did in our research (Supriyanti *et al.*, 2015, 2016, 2017a-c 2018a-c), we applied digital image processing techniques

to explore object variables before we do pattern recognition to classify these objects. In this study, we propose a classification using the ROC curve. We use the ROC curve in the initial classification due to its simple usage. In this study, we only discuss the pre-classification of the severity of Alzheimer's based on coronal slices morphology alone, so, there is no need for complex methods. This initial classification is to separate the images that will be explored in subsequent research.

MATERIALS AND METHODS

Data acquisition: The whole input images in this experiment used data from the Open Access Series of Imaging Studies (OASIS). Oasis is a project that aims to create a neuroimaging database and can be used freely in the research community and currently already published (Morris, 1993; Buckner *et al*., 2004; Rubin *et al*., 1998; Zhang *et al*., 2001; Fotenos *et al*., 2005). As we explained above in this study we discuss about classifying Alzheimer's severity on coronal slice only. Figure 2 shows examples of input images used in this experiment as already provided by OASIS database sets.

Image segmentation: In this experiment, we use the active contour method in image segmentation. The object that is segmented is ventricle and hippocampal. Some of the segmentation results have been published in our previous research by Supriyanti *et al.* (2018a-c). Based on the segmentation of the two objects, we explored the morphology of the two objects to be used as the initial determinant variable for the severity of Alzheimer's by using the ROC curve. Alzheimer's severity scale is determined based on Clinical Dementia Rating (CDR) which is commonly used in medical fields (Morris, 1993).

Receiver Operating Characteristic (ROC): ROC is a measurement in a diagnostic test to measure the performance of a device or system. One example in the medical field is comparing a new tool with standard medical equipment that is already standard. The main component in using ROC is calculating the False Positive (FP) and False Negative (FN) ratios on the segmentation results by comparing the results of the trial image segmentation in the original image. In identifying using ROC, suppose there is a classifier problem with two classes. Suppose that each pair of data I maps a set of elements {p, n} as a positive class label and a negative class label. The classification model maps the pair of data to the predicted class. To distinguish the actual class from

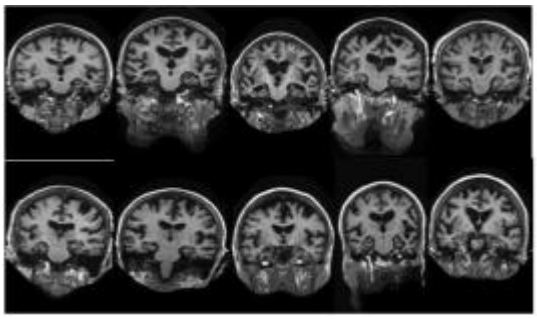

Fig. 2: Examples of input images (OASIS database sets)

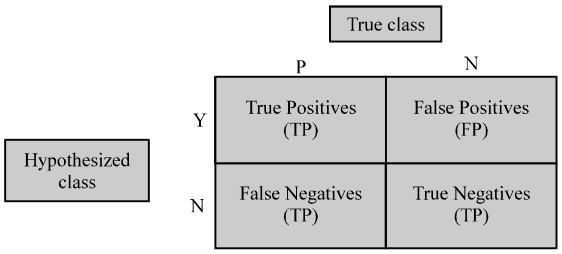

Fig. 3: Confusion matrix (Fawcett, 2006)

the predicted class, the predicted class is symbolized by {Y, N} (Fawcett, 2006). In terms of identifying images with Alzheimer's (AD) and healthy images, mapping will produce four outputs, namely TP, TN, FP and FN. Unlike the evaluation parameters for pixel segmentation, TP in identification is image data diagnosed by doctors as an image with AD, correctly detected AD after testing hypotheses whereas FP is image data with a healthy diagnosis but indicated as wrong with AD after testing, TN is an image data that is diagnosed by a doctor as a healthy image, detected correctly after going through hypothesis testing and FN is image data with a diagnosis of illness but indicated as wrong as a healthy image after testing these four values form a matrix called confusion matrix in Fig. 3. The parameters that will be used in ROC-based performance measurement are as follows:

Sensitivity: Sensitivity is a measure of the accuracy of the test, namely how likely the test is to detect positively the illness of people who have certain diseases or conditions. A test with high sensitivity will almost always be positive for people who have that condition (the test has a low false negative value). Sensitivity is also known as a true positive level and described in Eq. 1:

$$\text{Sensitivity (Se)} = \frac{TP}{TP+PN} = \frac{TP}{nD} \quad (1)$$

Specificity: Specificity is a measure of the accuracy of the test which is how likely the test to detect healthy negative people is declared healthy in certain conditions. A test with high specificity will almost always be negative for people who have that condition (the test has a low false positive value). Sensitivity is also known as true negative level or true negative rate and described in Eq. 2:

$$\text{Specificity (Sp)} = \frac{TN}{FP+TN} = \frac{TN}{nC} \quad (2)$$

Accuracy: Accuracy is the ratio of truth found in the results of a scientific study and described in Eq. 3:

$$\text{Accuracy} = \frac{TP+TN}{TP+TN+FP+fN} \quad (3)$$

Positive Predictive Value (PPV): Positive predictive value is the possibility that people with positive test results (image of being declared ill) will actually have the condition tested. The higher the positive predictive value (for example, 90%), the more useful the test is to predict that someone has the condition (Eq. 4):

$$PPV = \frac{TP}{(TP+FP)} = \frac{TP}{nP} \quad (4)$$

Negative Predictive Value (NPV): Negative predictive value is the possibility that people with negative test results (image declared healthy) do not have that condition. The higher the negative predictive value (for example, 99%), the more useful it is to predict that people do not have the condition (Eq. 5):

$$NPV = \frac{TN}{TN+FN} = \frac{TN}{nN} \quad (5)$$

The ROC curve is a comparison graph between sensitivity (TPR) on the vertical axis, namely the proportion of positive data that is correctly identified and specificity (FPR) on the horizontal axis, namely the proportion of negative data identified as being positive in a classification model (Fawcett, 2006). The ROC curve shows a trade off between the levels at which a model can accurately recognize positive data and the degree to which the model incorrectly identifies negative data as positive data.

RESULTS AND DISCUSSION

As we did in our previous research that prior to identifying using ROC, we performed image pre-processing stages which included image quality improvement and segmentation of the ventricular and hippocampal areas (Supriyanti *et al*., 2018). Figure 4 is an example of the results of ventricular and hippocampal segmentation using the active contour method. Figure 4 is an example of the results of ventricular and hippocampal segmentation using the active contour method.

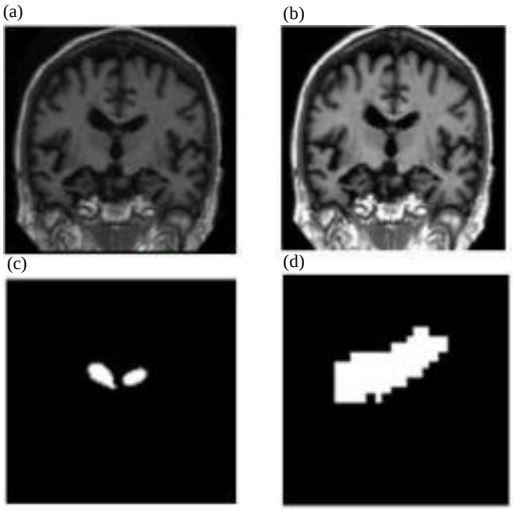

Fig. 4: An example of object segmentation: a) Orinal image; b) Results of pre-processing; c) Ventricular segmentation and d) Hippocampal segmentation

Based on the results of the segmentation then automatically measuring the area width for each object using the tools we have made using MATLAB programming. Figure 5 and 6 show the results of the FP and FN ratios for ventricular and hippocampal objects.

The FP ratio is the ratio between pixels that should not be vessels in the reference image but segmented as vessel pixels. The FN ratio is the ratio between pixels that should be part of the brain vessels but segmented as non-vessels with pixels from reference images. According to Fig. 5 in the image with AD, the FP ratio shows a value greater than the FN ratio and the FP ratio graph decreases as the number of pixels decreases from the test image. This shows that objects with AD diagnosis have more pixels than reference objects, so, the FP ratio is large. Conversely, objects with healthy diagnoses have fewer pixels than reference objects, so, the false positive ratio is very small. In the image with AD, the FN ratio shows a smaller value than the FP ratio and the FN ratio graph increases as the number of pixels decreases from the test image. This shows that objects with AD diagnosis have more pixels than reference objects, so, the FN ratio is small. Conversely, objects with healthy diagnoses have

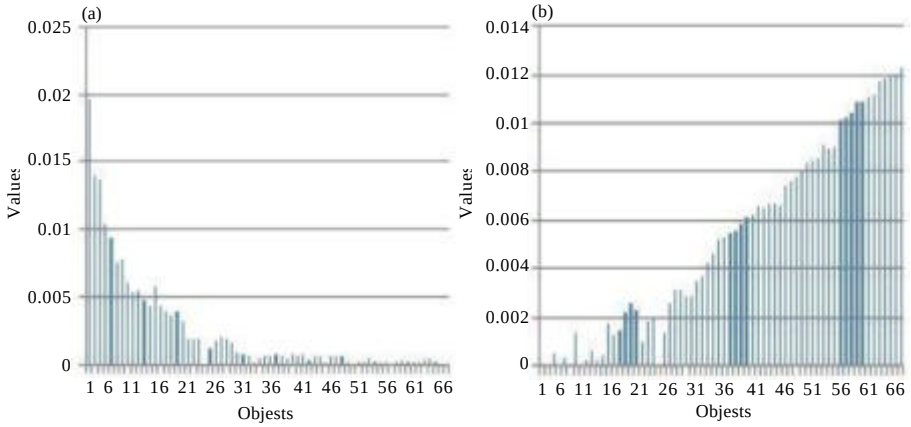

Fig. 5: Ratio of FP and FN for Hippocampal objects: a) FP ratio and b) FN ratio

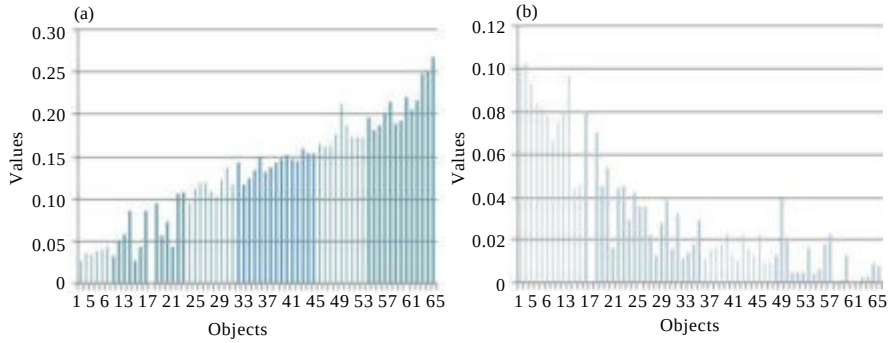

Fig. 6: Ratio of FP and FN for Hippocampal objects a) FP ratio and b) FN ratio

Table 1: Confusion matrix for ventricular objects

Variables	Alzheimer disease (D)	Healthy (C)	Total
Test positive	TP = 14	FP = 8	nP = 22
Tes negative	FN = 1	TN = 43	nN = 45
Totl	nD = 15	nC = 51	N = 66

Table 2: ROC parameter values for ventricular objects

ROC parameter	Values
Sensitivity	0.934
Specificity	0.843
Accuracy	0.863
PPV	0.636
NPV	0.977

fewer pixels than reference objects so the false negative ratio is very large. Whereas in hippocampal objects, the FP and FN ratios are the opposite of ventricular objects as described in Fig. 6.

In terms of image identification with AD and healthy image, mapping will produce ROC parameter values. TP which is the image data diagnosed by the doctor as an image with AD, detected AD correctly after going through testing on 14 ventricular objects, FP that is an image with a healthy diagnosis but indicated wrong as an image with AD after testing, giving a value of 8 images, TN is the image data diagnosed by the doctor as a healthy image and detected healthy correctly after going through hypothesis testing, valued at 43 and FN namely image data with AD diagnosis but indicated as wrong as a healthy image after testing is 1. Confusion matrix is shown in Table 1. The total Positive number (nP) is 22, the total number of Negative (nN) is 45, nD or the total number of images with AD is 15 and nC or the total number of healthy images is 51. Overall sample images (TP+FP+FN+TN) is 66. While the ROC parameter values for ventricular objects are shown in Table 2.

Table 3: Confusion matrix for hippocampal objects

Variables	Alzheimer disease (D)	Healthy (C)	Total
Test positive	TP = 15	FP = 1	nP = 16
Tes negative	FN = 0	TN= 50	nN = 50
Total	nD = 15	nC = 51	N = 66

Referring to Table 2, the ROC curve for ventricular objects can be made as shown in Fig. 7. Referring to Fig. 7, the AUC value is between 0.80 and 0.90, the system performance is "Good". While confusion matrix and ROC parameter values for hippocampal objects are shown in Table 3 and 4.

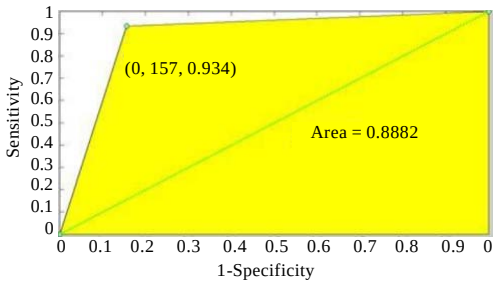

Fig. 7: ROC curve for ventricular objects

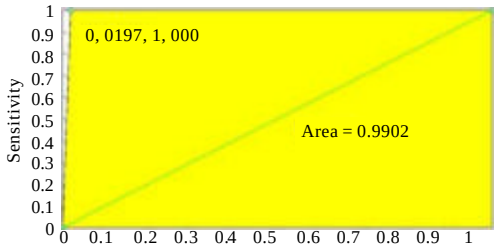

Fig. 8: ROC curve for Hippocampal objects

Table 4: ROC parameter values for Hippocampal objects

ROC parameter	Values
Sensitivity	1
Specificity	0.9803
Accuracy	0.9804
PPV	0.9375
NPV	1

Table 5: Results of identification between healthy image and image with AD

Object segmentation	Images with AD (CDR 0) (pixels)	Healthy images (CDR 1-2) (pixels)	AUC	Classification
Ventricular	50-472	473-899	0.8882	Good
Hippocampal	68-138	148-296	0.9902	Excellent

Referring to Table 4, the ROC curve for hippocampal objects are shown in Fig. 8. The AUC value of 0.9902, being between 0.90 and 1.0 then the system performance is "Excellent".

Thus, identification of ventricular objects can be done with a sensitivity value of 0.934 and a specificity of 0.84, identification of hippocampal objects can be done with a very high sensitivity value of 1 and also a high specificity of 0.9803. Identification performance on ventricular objects is "Good" and "Excellent" for identification of hippocampal objects of Alzheimer's patients. This is indicated by Table 5 which is reviewed based on the Area Under Curve (AUC) ratio.

CONCLUSION

The FP ratio of the healthy image ventricular object has an average value that is smaller than the healthy image FN ratio which is the FP ratio of 0.001 and the FN ratio of 0.006, indicating the characteristics of the healthy lateral ventricular object has a narrow area. The FP ratio of image ventricular objects with AD has a higher value than the FN ratio of 0.005 and the FN ratio of 0.001. The characteristics of image ventricular objects with AD have a wider area than the reference image. The FP ratio of the healthy image hippocampal object has an average value that is greater than the healthy image FN ratio, i.e., the FP ratio is 0.15 and the FN ratio is 0.01, indicating the characteristics of the healthy image hippocampus object has a wide area. The FP ratio of the image hippocampus object with AD has a lower value than the FN ratio of 0.04 and a FN ratio of 0.07, indicating that the characteristics of the image hippocampal object with AD have an area that is narrower than the reference image. Pixel-based identification is taken from the largest pixel value of the image with the hippocampal AD object which is 138 pixels and the smallest value of the ventricular object pain image is 473 pixels. Testing the results of identification through ROC parameters gives an accuracy value of 86.3% for the ventricular area. While for hippocampus area objects, identification can be done with 98.4% accuracy. Area Under Curve (AUC) ventricular object is 0.8882 with the classification "Good" while the AUC hippocampus object has an area of 0.9902 with the classification "Excellent".

ACKNOWLEDGEMENTS

We Thank the Open Access Series of Imaging Studies (OASIS) datasets and in the associated PubMed Central submission: P50 AG05681, P01 AG03991, R01 AG021910, P50 MH071616, U24 RR021382, R01 MH56584. This Research is supported by the Ministry of Research, Technology and Higher Education Indonesia through "Hibah Penelitian Berbasis Kompetensi" Scheme.

REFERENCES

Belloy, M.E., D. Shah, A. Abbas, A. Kashyap and S. Roßner *et al*., 2018. Quasi-periodic patterns of neural activity improve classification of Alzheimer's disease in Mice. Sci. Rep., 8: 1-15.

Buckner, R.L., D. Head, J. Parker, A.F. Fotenos and D. Marcus *et al*., 2004. A unified approach for morphometric and functional data analysis in young, old and demented adults using automated atlas-based head size normalization: reliability and validation against manual measurement of total intracranial volume. Neuroimage, 23: 724-738.

Cho, Y., J.K. Seong, Y. Jeong and S.Y. Shin, 2012. Individual subject classification for Alzheimer's disease based on incremental learning using a spatial frequency representation of cortical thickness data. Neuroimage, 59: 2217-2230.

Dyrba, M., M. Ewers, M. Wegrzyn, I. Kilimann and C. Plant *et al*., 2013. Robust automated detection of microstructural white matter degeneration in Alzheimer's disease using machine learning classification of multicenter DTI data. PloS One, 8: 1-14.

Fawcett, T., 2006. An introduction to ROC analysis. Pattern Recognit. Lett., 27: 861-874.

Fiscon, G., E. Weitschek, A. Cialini, G. Felici and P. Bertolazzi *et al*., 2018. Combining EEG signal processing with supervised methods for Alzheimer's patients classification. BMC. Med. Inf. Decis. Making, 18: 1-10.

Fotenos, A.F., A.Z. Snyder, L.E. Girton, J.C. Morris and R.L. Buckner, 2005. Normative estimates of cross-sectional and longitudinal brain volume decline in aging and AD. Neurol., 64: 1032-1039.

Fu, L., L. Liu, J. Zhang, B. Xu and Y. Fan *et al*., 2014. Comparison of dual-biomarker PIB-PET and dual-tracer PET in AD diagnosis. Eur. Radiol., 24: 2800-2809.

Gerardin, E., G. Chételat, M. Chupin, R. Cuingnet and B. Desgranges *et al*., 2009. Multidimensional classification of hippocampal shape features discriminates Alzheimer's disease and mild cognitive impairment from normal aging. Neuroimage, 47: 1476-1486.

Gray, K.R., R. Wolz, R.A. Heckemann, P. Aljabar and A. Hammers *et al*., 2012. Multi-region analysis of longitudinal FDG-PET for the classification of Alzheimer's disease. NeuroImage, 60: 221-229.

Huang, M., W. Yang, Q. Feng and W. Chen, 2017. Longitudinal measurement and hierarchical classification framework for the prediction of Alzheimer's disease. Sci. Rep., 7: 1-13.

Morris, J.C., 1993. The Clinical Dementia Rating (CDR): Current version and scoring rules. Neurol., 43: 2412-2414.

Rubin, E.H., M. Storandt, J.P. Miller, D.A. Kinscherf and E.A. Grant *et al*., 1998. A prospective study of cognitive function and onset of dementia in cognitively healthy elders. Arch. Neurol., 55: 395-401.

Singanamalli, A., H. Wang and A. Madabhushi, 2017a. Cascaded Multi-view Canonical Correlation (CaMCCo) for early diagnosis of alzheimer's disease via fusion of clinical, imaging and Omic features. Sci. Rep., 7: 1-15.

Supriyanti, R., A. Chrisanty, Y. Ramadhani and W. Siswandari, 2018. Computer aided diagnosis for screening the shape and size of leukocyte cell nucleus based on morphological image. Intl. J. Electr. Comput. Eng., 8: 150-158.

Supriyanti, R., A. Fariz, T. Septiana, E. Murdyantoro and Y. Ramadhani *et al*., 2015. Simple screening for high-risk pregnancies in rural areas based on an expert system. Telecommun. Comput. Electr. Control, 13: 661-669.

Supriyanti, R., A.A. Hafidh, Y. Ramadhani and H.B. Widodo, 2018c. Measuring gestational age and uterine diameter based on image segmentation. ARPN. J. Eng. Appl. Sci., 13: 670-676.

Supriyanti, R., A.R. Subhi, Y. Ramadhani and H.B. Widodo, 2018b. Calculating ventricle's area based on Clinical Dementia Rating (CDR) values on coronal MRI image. Proceedings of the 20th International Conference on Computer-Based Patient Records and Error Prevention (ICCPREP), August 20-21, 2018, World Academy of Science, Engineering and Technology, London, UK., pp: 164-164.

Supriyanti, R., A.S. Setiadi, Y. Ramadhani and H.B. Widodo, 2016. Point processing method for improving dental radiology image quality. Intl. J. Electr. Comput. Eng., 6: 1587-1594.

Supriyanti, R., G.P. Satrio, Y. Ramadhani and W. Siswandari, 2017b. Contour detection of leukocyte cell nucleus using morphological image. J. Phys. Conf. Ser., 824: 1-9.

Supriyanti, R., S.A. Priyono, E. Murdyan and H.B. Widodo, 2017c. Histogram equalization for improving quality of low-resolution ultrasonography images. Telkomnika, 15: 1397-1408.

Tohka, J., E. Moradi and H. Huttunen, 2016. Comparison of feature selection techniques in machine learning for anatomical brain MRI in dementia. Neuroinf., 14: 279-296.

Wee, C.Y., P.T. Yap, K. Denny, J.N. Browndyke and G.G. Potter *et al*., 2012. Resting-state multi-spectrum functional connectivity networks for identification of MCI patients. PloS One, 7: 1-11.

Wolz, R., V. Julkunen, J. Koikkalainen, E. Niskanen and D.P. Zhang *et al*., 2011. Multi-method analysis of MRI images in early diagnostics of Alzheimer's disease. PloS One, 6: e25446-e25446.

Ye, T., C. Zu, B. Jie, D. Shen and D. Zhang, 2016. Discriminative multi-task feature selection for multi-modality classification of Alzheimer's disease. Brain Imaging Behave., 10: 739-749.

Yun, H.J., K. Kwak and J.M. Lee, 2015. Multimodal discrimination of Alzheimer's disease based on regional cortical atrophy and hypometabolism. PloS One, 10: 1-19.

Zhang, Y., M. Brady and S. Smith, 2001. Segmentation of brain MR Images through a hidden markov random field model and the Expectation-Maximization algorithm. IEEE Trans. Medi. Imag., 20: 45-57.